

Right Ventricle Involvement by Glycogen Storage Cardiomyopathy (PRKAG2): Standard and Advanced Echocardiography Analyses

José Luiz Barros Pena,^{1,2}^{ID} Fabricio Junqueira de Melo,¹ Wander Costa Santos,¹ Isabel Cristina Gomes Moura,¹ Gabriela Pansanato Nakashima,¹ Natália Costa Freitas,¹ Eduardo Back Sternick¹

Faculdade de Ciências Médicas de Minas Gerais – Pós-Graduação,¹ Belo Horizonte, MG – Brazil

Hospital Felício Rocho – Ecocardiografia,² Belo Horizonte, MG – Brazil

Abstract

Background: PRKAG2 syndrome is a rare, early-onset autosomal dominant inherited disease. We aimed to describe the right ventricle (RV) echocardiographic findings using two and three-dimensional (2D and 3D) modalities including myocardial deformation indices in this cardiomyopathy. We also aimed to demonstrate whether this technique could identify changes in RV function that could distinguish any particular findings.

Methods: Thirty patients with genetically proven PRKAG2 (R302Q and H401Q), 16 (53.3%) males, mean age 39.1 ± 15.4 years, underwent complete echocardiography examination. RV-focused, 4-chamber view was acquired for 2D and 3D measurements. Student's t or Wilcoxon-Mann-Whitney tests were used to compare numerical variables between 2 groups, and $p < 0.05$ was considered significant.

Results: Twelve patients (40%) had a pacemaker implanted for 12.4 ± 9.9 years. RV free wall mean diastolic thickness was 7.9 ± 2.9 mm. RV 4-chamber longitudinal strain (RV4LS), including the free wall and interventricular septum, was $-17.3\% \pm 6.7\%$, and RV free wall longitudinal strain (RVFWLS) was $-19.1\% \pm 8.5\%$. The RVFWLS apical ratio measured 0.63 ± 0.15 . Mean RV 3D ejection fraction (EF) was $42.6\% \pm 10.9\%$ and below normal limits in 56.7% of patients. Positive correlation occurred between RV 3DEF, RV4LS, and RVFWLS, especially for patients without a pacemaker ($p = 0.006$).

Conclusion: RV involvement in PRKAG2 syndrome is frequent, occurring in different degrees. Echocardiography is a valuable tool in detecting RV myocardial abnormalities in this condition. The use of 2D RV4LS, RVFWLS, and 3DEF offers reliable indicators of RV systolic dysfunction in this rare, challenging cardiomyopathy.

Keywords: PRKAG2 Syndrome/genetics; Glycogen Storage Disease/complications; Hypertrophy, Right Ventricular; Cardiomyopathy, Hypertrophic Familial; Echocardiography/methods; Pacemaker, Artificial; Stroke Volume.

Introduction

The PRKAG2 gene was initially described in 2000 as an active part of metabolism in the transcription process of AMP-activated protein kinase (AMPK).^{1,2} In nearly half of the reported cases, genomic changes involving this gene are due to the Arg302Gln mutation, which replaces arginine with glutamine at codon 302, known as R302Q. The literature also describes 28 additional mutations.³ The PRKAG2 mutation results in loss of function of the $\gamma 2$ subunit of AMPK and features a metabolic defect responsible for glycogen metabolic disease. The main phenotype consists of ventricular hypertrophy associated with abnormalities in the cardiac conduction system, including ventricular pre-excitation syndrome.⁴

PRKAG2 mutation is considered a rare disease, although it is probably underestimated, because many cases are improperly diagnosed, often being labeled as familial sarcomeric hypertrophic cardiomyopathy. The inheritance pattern is dominant, with complete penetrance and varying degrees of expression and prevalence still unmentioned in the literature.^{5,6}

Two- and three-dimensional (2D and 3D) echocardiography and myocardial deformation indices (strain/strain rate) by speckle tracking (STE) are relatively recent techniques, yet they are already used for assessing left ventricle (LV) function. More recently, these techniques have also been validated for assessing right ventricle (RV) function.^{7,8}

Our research group recently published a study of the LV echocardiography findings in this same series of patients.⁹

The recognized importance of the RV in cardiomyopathies is radically changing, and this significantly affects cardiac physiology, hemodynamics, and the development of symptoms.¹⁰ Compared to systemic circulation, pulmonary circulation has a much lower vascular resistance and greater pulmonary artery distensibility.¹¹⁻¹⁴

Mailing Address: José Luiz Barros Pena •

Faculdade de Ciências Médicas de Minas Gerais – Pós-Graduação – Alameda Ezequiel Dias, 275. Postal code 30130-110, Belo Horizonte, MG – Brazil

E-mail: jlbpena@cardiol.br

Manuscript received September 18, 2021, revised manuscript April 27, 2022, accepted June 15, 2022

DOI: <https://doi.org/10.36660/abc.20210801>

We aim to describe the RV echocardiographic findings using 2D and 3D echocardiography and STE. We also aim to identify if this technique could eventually detect any particular changes in RV function in glycogen storage cardiomyopathy when compared to LV. As little research exists associating RV echocardiographic findings with PRKAG2 syndrome, we seek to investigate the presence of echocardiographic parameters that could suggest RV hypertrophy associated with glycogen deposit cardiomyopathy.

Methods

Patients and study protocol

This is an observational, clinical, transversal study, based on a cohort of patients with genetically proven PRKAG2 syndrome. Patients with other hypertrophic cardiomyopathy etiologies were excluded. The target population consisted of 30 patients from 5 families with PRKAG2 gene mutation (28 Arg302Gln and 2 His401Gln), detected utilizing Sanger sequential genetic testing. All patients underwent clinical examination, with a standard 12-lead electrocardiogram and echocardiogram. The institutional review board approved the protocol and all patients signed a written informed consent form. Our study was performed following the guidelines of Good Clinical Practice and was approved by the local ethics committees.

Echocardiographic analysis

All patients underwent a complete transthoracic echocardiography examination, following the recommendations of the American Society of Echocardiography (ASE) and the European Association of Cardiovascular Imaging (EACVI).¹⁵ All studies were performed using a commercially available echocardiographic system, Vivid E9 machine (GE Healthcare, Horten, Norway). The examination included M-mode, 2D measurements, 2D STE of longitudinal strain, and 3D measurements according to The Guidelines for the Echocardiographic Assessment of the Right Heart in Adults: a report from the ASE.¹⁶ The RV-focused, 4-chamber view was acquired for 2D and 3D measurements, and care was taken to obtain the image demonstrating the maximum diameter. RV 2D linear dimensions were measured, including RV basal, mid-cavity, and longitudinal dimensions. The RV outflow tract was measured at end-diastole in the parasternal long-axis view. RV wall thickness was measured in diastole, from the subcostal view, using M-mode imaging.

Tricuspid annular plane systolic excursion (TAPSE) was obtained by M-mode, measured from the tricuspid lateral annulus.

Inferior vena cava was measured proximal to the junction of the hepatic veins at end-expiration. RV 4-chamber longitudinal strain (RV4LS) was calculated by averaging values of all 6 RV segments. RV free wall longitudinal strain (RVFWLS) was obtained by averaging the 3 free wall RV segments: basal, mid, and apical. We also calculated the RVFW apical ratio using the equation:

[apical peak systolic longitudinal strain (PSLS) / (basal PSLS + mid-PSLS)]. All data were reviewed offline. RV transthoracic 3D echocardiography was performed in all patients. Six electrocardiogram-gated consecutive beats were acquired to generate the full RV volume. Post-processing of real-time 3D images was performed using TomTec software 1.1, with the endocardial tracing of all planes. RV volumes were semi-automatically computed throughout the entire cardiac cycle, from which end-diastolic volume and end-systolic volume were obtained, and stroke volume and ejection fraction (EF) were calculated. Intra- and interobserver reproducibility were assessed on a subsample of 9 randomly selected patients.

Statistical analysis

The sample sized used was a convenience sample due to the rarity of this condition. Categorical variables were presented by absolute and relative frequencies and numerical variables as mean \pm standard deviation if normally distributed and median \pm interquartile range if abnormally distributed. The normality of the numerical variables was assessed using the Shapiro-Wilk test. Student's t or Wilcoxon-Mann-Whitney tests were used to compare numerical variables between 2 groups used for independent samples. The association between categorical variables was assessed using Fisher's exact test. Spearman's correlation coefficient was used to assess the association between 2 numerical variables.

The 30 cases were randomly assigned numbers from 1 to 30 using R software. To assess consistency and reproducibility, 2 independent observers randomly selected 9 numbers for remeasurement. The choice for the number of cases was arbitrary.

Mean differences and intraclass correlation coefficients (ICC) were obtained. Their intra- and interobserver confidence intervals (CI) were both 95%. Intra- and interobserver measurements were assessed using the Shapiro-Wilk test. Student t-tests for paired samples were used to compare mean differences.

The analyses were performed using R software version 3.5.2, and $p < 0.05$ was considered significant.

Results

Table 1 shows the clinical and demographic characteristics of the patients in the study. The majority were male, and more than half were asymptomatic. Palpitation was the most frequent clinical symptom. Pre-excitation syndrome, hypertension, and flutter were prevalent signs.

RV echocardiographic parameters are listed in Table 2. The 3D image quality was inadequate in 2 patients.

It is important to report that, during the echocardiogram, only 1 patient presented atrial fibrillation. Measured by the subcostal view using M-mode, RV lateral wall median diastolic thickness was 7.0 ± 3.0 mm (Figure 1). Only 3 patients presented normal values, and, in 1 patient, the measurement reached 20 mm. Only 3 patients showed TAPSE values below 17 mm.

Table 1 – Clinical and demographic characteristics of patients

Population, n = 30	
Male	16 (53.3%)
Age (years)*	39.1 ± 15.2
BMI (kg/m ²)*	26.9 ± 3.8
BSA (m ²)*	1.8 ± 0.2
Heart rate (bpm)**	60.0 (53.0 – 63.0)
Blood pressure	
Systolic (mmHg)**	120.0 (112.5 – 130.0)
Diastolic (mmHg)**	77.5 (70.0 – 80.0)
Signs and symptoms	
Pre-excitation	19 (63.3%)
Asymptomatic	16 (53.3%)
Pacemaker	12 (40%)
Hypertension	10 (33.3%)
Palpitations	7 (23.3%)
Flutter	6 (20%)
AF	4 (13.3%)
Shortness of breath	2 (6.7%)
Presyncope	2 (6.7%)

AF: atrial fibrillation; BMI: body mass index; BSA: body surface area; bpm: beats per minute. Data showed as * mean ± standard deviation, ** median (1st – 3rd quartile).

Parasternal long-axis anterior portion of RV outflow tract dimension at the proximal level presented higher values compared to normal in 23% of patients, as reported in the literature, except for the longitudinal dimension. This value suggests that the RV chamber increase occurred in the transverse section.

Tricuspid regurgitation was detected in half of patients, but only 4 presented pulmonary artery systolic pressure above normal limits, and the maximum estimated value reached 48 mmHg.

Inferior vena cava was dilated in only 2 patients.

In 3 patients, RV4LS was significantly reduced, relating to more thickened lateral wall (Figure 2).

Table 2 also shows the mean RVFWLS values of each segment. We can observe that the RVFWLS basal values are lower than medial ($p = 0.016$) and apical segments ($p < 0.001$).

RVEF was within normal limits in 13 patients and below 35% in 7 patients (Figure 3).

Patients with a pacemaker (PM) were significantly older ($p < 0.001$), and they had a higher proportion of atrial fibrillation compared to patients without PM ($p = 0.018$). The pacemaker was implanted at 38.1 ± 13 years, and the median time of use was 12.4 ± 9.9 years.

Table 2 – Echocardiographic RV parameters of 30 patients

Variable	
RVFW thickness (mm)**	7.0 (6.0 – 9.0)
TAPSE (mm)*	18.8 ± 3.7
RV basal cavity diameter (mm)*	37.6 ± 5.7
RV mid cavity diameter (mm)*	31.0 ± 6.1
RV longitudinal diameter (mm)**	49.0 (35.0 – 61.0)
RVOT PLAX diameter (mm)*	28.0 ± 4.0
IVC at end-expiration (mm)**	17.0 (16.0 – 19.0)
RV4LS (%) **	-18,8 (-14,0 – 20,9)
RVFWLS (%) **	-20.3 (-16.6 – 25.3)
RVFW basal LS (%) *	-18.0 ± 5.1
RVFW mid LS (%) *	-21.8 ± 5.8
RVFW apical LS (%) *	-24.3 ± 7.1
RV apical ratio*	0.63 ± 0.15
RV 3D EDV (mL) **	95.2 (76.2 – 129.9)
RV 3D ESV (mL) **	54.0 (44.8 – 69.6)
RV 3D SV (mL) **	44.6 (30.4 – 59.6)
RV 3D EF (%) *	42.6 ± 10.9

EDV: end-diastolic volume; EF: ejection fraction; ESV: end-systolic volume; IVC: inferior vena cava; PLAX: parasternal long-axis; RV: right ventricle; RV4LS: right ventricle longitudinal strain; RVFW: right ventricle free wall; RVFWLS: right ventricle free wall longitudinal strain; RVOT: right ventricular outflow tract; SV: stroke volume; TAPSE: tricuspid annular plane systolic excursion; 3D: three-dimensional. Data showed as * mean ± standard deviation, ** median (1st – 3rd quartile).

Patients with PM presented significantly lower values of 3D LVEF, fractional shortening, and 3D global circumferential strain.

We detected a statistically significant difference between measurements of RVFWLS basal and mid-segment between patients with and without PM, as shown in Table 3.

However, no other significant differences appeared among the RV echocardiographic findings between patients with and without PM.

The correlations between the strain variables and RVEF were assessed, as shown in Table 4. A positive correlation occurred between EF and RVFWLS ($r = 0.65$, $p = 0.006$), indicating that the higher the absolute value of RVFWLS, the higher the EF values. Considering RV4LS, correlation was lower in all patients and absent in patients with PM.

We also found a positive correlation between the reduction of LVEF and RVFWLS (less than 50% and -18%, respectively) ($r = 0.80$, $p = 0.05$).

The reproducibility of strain and 3D measurements, and the ICC and CI for inter- and intraobserver variability are summarized in Table 5.

Discussion

Mutations in the PRKAG2 gene alter AMPK homeostasis, and the echocardiographic assessment of patients with the mutation is an opportunity to assess the potential long-term systemic consequences of AMPK activation. By assessing these consequences, new lines of research could indicate metabolic pathways involved in the disease pathophysiology leading to partial or total phenotype recognition.¹⁷ PRKAG2 syndrome has different cardiac phenotypes, ranging from an asymptomatic condition to sudden cardiac death, including

biventricular hypertrophy, pre-excitation, atrioventricular conduction abnormalities, atrial flutter, and fibrillation.^{18,19}

A large multicenter European cohort was recently published reporting data from 90 patients with PRKAG2 variants.²⁰ This study showed that patients with PRKAG2 genetic variants have a poor prognosis with a high rate of complications, including juvenile onset of conduction disease, advanced HF, and potentially lethal arrhythmias.

Evaluation of RV size and systolic performance is increasingly in demand due to its recognizable significance and prognosis, especially in hypertrophic cardiomyopathy, arrhythmogenic RV cardiomyopathy, and amyloidosis.²¹ To the best of our knowledge, this research represents the largest RV echocardiographic study in a population with PRKAG2 mutation. We aimed to describe the RV findings in this rare genetic disorder and the occurrence of dysfunction, incidence, and degree of dysfunction.

The RV was affected in the great majority of patients. RV hypertrophy occurred in 90% of patients, presented a regular pattern, involved all portions of the chamber, and reached 20 mm in 1 case. This finding is similar to other infiltrative or genetic diseases.^{22,23} Rosca et al.²³ related that patients with hypertrophic cardiomyopathy had increased RV wall thickness compared to controls with increased calculated sudden cardiac death risk.²³

We evaluated these patients' myocardial deformation (RV4LS and RVFWLS), RV volumes, and EF. We found that the RVFWLS of basal segments showed lower values than mid and apical segments. However, the RVFW ratio showed that the RV strain analyses presented no apical

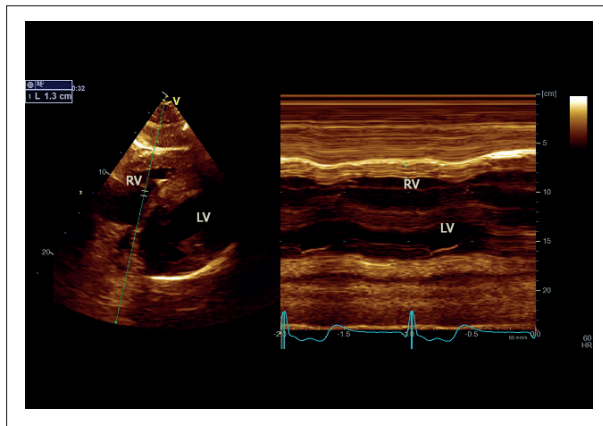


Figure 1 – Measurement of end-diastolic right ventricle free wall thickness. Subcostal 2-dimensional image of the 4-chamber view. M-mode image indicating wall thickness at end-diastole (1.3 cm). LV: left ventricle; RV: right ventricle.

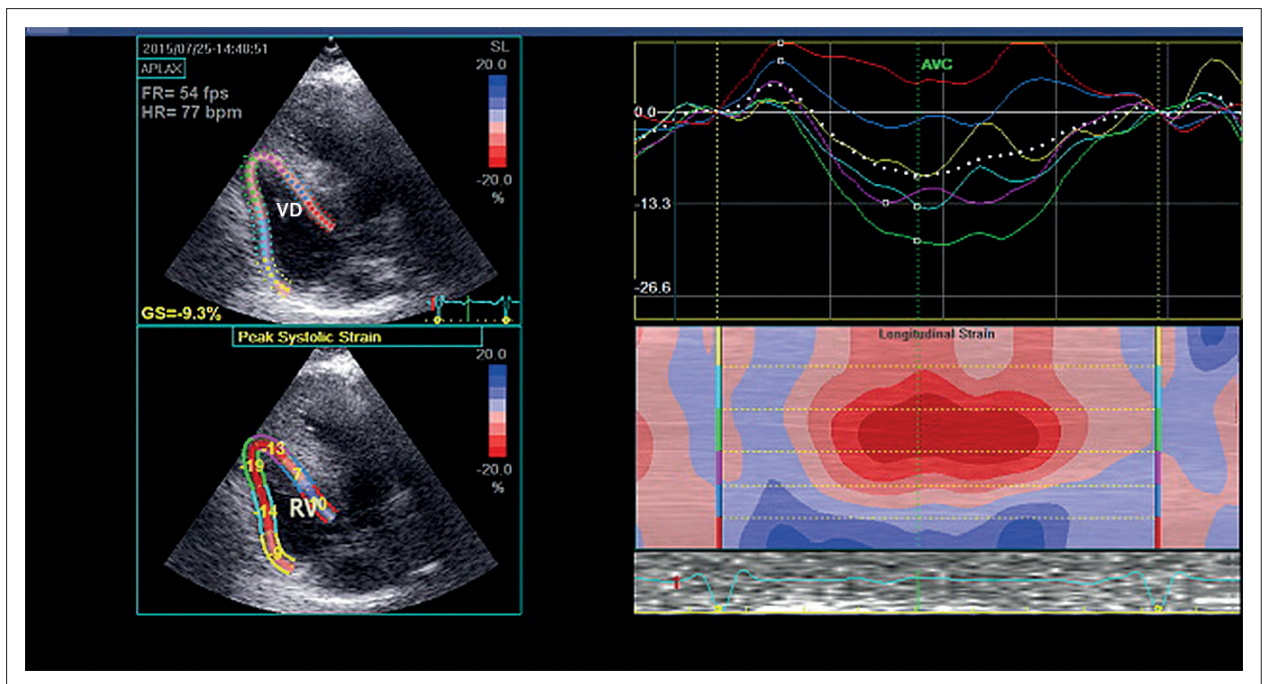


Figure 2 – Two-dimensional speckle tracking analysis of the right ventricle from a focused apical 4-chamber view. The global average systolic strain values and time curves are obtained by tracking of a 6-segment region of interest. Right ventricle 4-chamber longitudinal strain measured 9.3%. GS: global strain; RV: right ventricle.

sparing pattern, as described in systemic light-chain cardiac amyloidosis.²⁴ It is noteworthy that RVFWLS was feasible in all patients.

We found that RVEF was below normal limits in more than half of patients (56.7%), and, in 7 patients, RVEF

was below 35%. These values were unaffected by PM, and they could indicate a differential signal of this disease when compared to other hypertrophic phenotypes. We considered normal RVEF $\geq 45\%$.⁸ Some patients (17.2%) also presented reduced LVEF, especially patients with

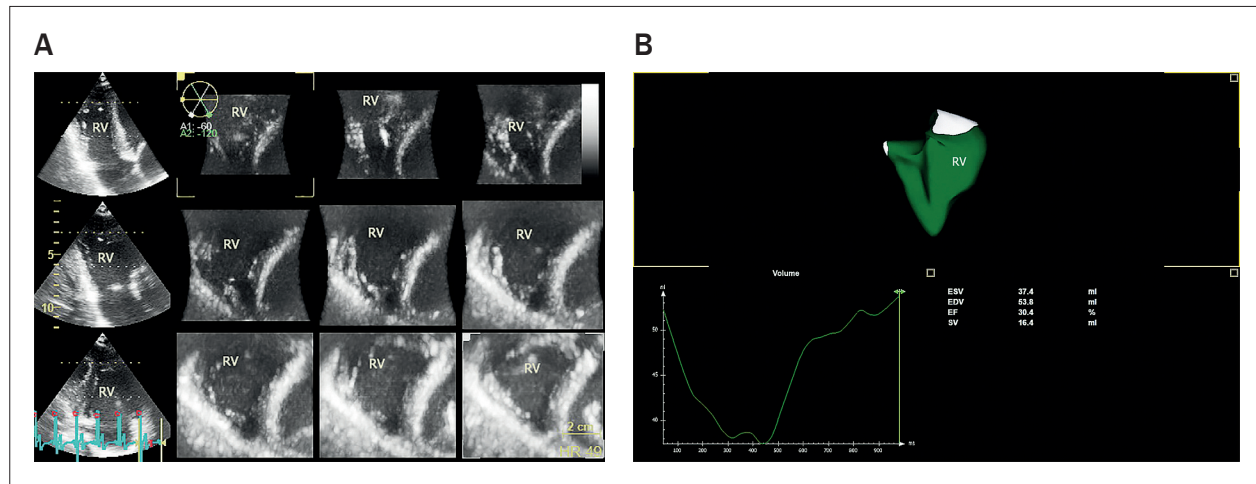


Figure 3 – The 3-dimensional dataset was acquired from an RV-focused apical 4-chamber view. In A, there is a multiplanar short-axis view to verify the endocardial borders. In B, we can see the RV 3-dimensional model obtained with the volume curve. EDV: end diastolic volume; EF: ejection fraction; ESV: end systolic volume; RV: right ventricle; SV: stroke volume.

Table 3 – Echocardiographic RV parameters of patients without and with pacemaker

Variable	Without PM (n=18)	With PM (n=12)	p-value
RVFW thickness (mm)**	7.0 (6.0 – 8.8)	8.0 (6.5 – 9.0)	0.233 ^W
TAPSE (mm)*	19.9 ± 2.9	17.0 ± 4.1	0.060 ^T
RV basal cavity diameter (mm)*	36.8 ± 4.7	39.0 ± 7.1	0.372 ^T
RV mid cavity diameter (mm)*	31.0 ± 5.4	31.1 ± 7.5	0.973 ^T
RV longitudinal diameter (mm)*	49.8 ± 13.4	49.0 ± 15.5	0.892 ^T
RVOT PLAX diameter (mm)*	27.0 ± 4.2	29.6 ± 3.3	0.088 ^T
IVC at end-expiration (mm)**	17.0 (16.0 – 18.8)	18.0 (16.5 – 19.5)	0.440 ^W
RV4LS (%) *	-18.5 ± 6.8	-13.0 ± 6.4	0.233 ^T
RVFWLS (%) **	-24.0 (-18.3 – -25.7)	-18.6 (-13.0 – 22.2)	0.187 ^W
RVFW basal LS (%) *	-19.7 ± 4.9	-15.6 ± 4.5	0.037 ^T
RVFW mid LS (%) **	-26.0 (-18.5 – -26.5)	-19.0 (-14.5 – -23.5)	0.039 ^W
RVFW apical LS (%) *	-25.8 ± 7.3	-22.2 ± 6.6	0.200 ^T
RV apical ratio*	0.61 ± 0.18	0.65 ± 0.11	0.458 ^T
RV 3D EDV (mL)**	95.7 (84.9 – 119.0)	92.9 (69.2 – 149.5)	0.746 ^W
RV 3D ESV (mL)**	56.0 (45.7 – 68.4)	51.5 (43.4 – 79.8)	0.963 ^W
RV 3D SV (mL)**	45.1 (36.2 – 59.2)	30.6 (29.3 – 59.4)	0.742 ^W
RV 3D EF (%) **	48.5 (36.7 – 51.6)	37.5 (32.8 – 40.6)	0.259 ^W

EDV: end-diastolic volume; EF: ejection fraction; ESV: end-systolic volume; IVC: inferior vena cava; PLAX: parasternal long-axis; PM: pacemaker; RV: right ventricle; RV4LS: right ventricle longitudinal strain; RVFW: right ventricle free wall; RVFWLS: right ventricle free wall longitudinal strain; RVOT: right ventricular outflow tract; SV: stroke volume; TAPSE: tricuspid annular plane systolic excursion; 3D: three-dimensional. Data showed as * mean ± standard deviation, ** median (1st – 3rd quartile). T Student's t and W Wilcoxon-Mann-Whitney test for independent samples.

PM. As previously reported, patients with PM presented significantly lower values of 3D LVEF, fractional shortening, and 3D global circumferential strain.²⁵

RVEF reduction occurred in a greater proportion of patients and will likely be a differential signal compared to other hypertrophic cardiomyopathies such as Fabry and Danon diseases.

Echocardiography is a practical, non-invasive technique to identify morphological and functional alterations in clinical practice.¹⁵

Even asymptomatic patients presented RV4LS and RVFWLS below normal reference limits. As the feasibility of 3D RV volume estimation has been proven in this syndrome, this method can be reliably applied in clinical diagnoses.^{26,27}

Echocardiography presents no harmful effects in patients with PM, and it has lower cost, higher portability, and easier reapplication than cardiac magnetic resonance.²⁸

We observed that conventional echocardiographic indices, like TAPSE, were unreliable indicators for RV dysfunction detection. In previous studies, with other infiltrative diseases, these indicators showed less sensitivity to detect functional myocardial alterations than RV 2D STE analyses.²⁷ Interestingly, by using Doppler, we detected no obstruction in the RV outflow tract at rest. A recently

published case report detected a dynamic biventricular outflow tract obstruction in a patient with a syncopal episode. Genetic testing revealed that the patient was heterozygous for R302Q missense mutation in the PRKAG2 gene, as in the majority of our cases.²⁶

We confirmed a positive correlation between RVFWLS and RVEF, with statistical significance. These findings indicate that the deformation indices are a fast and widely available method to detect dysfunction, comparable to 3D EF in patients with the PRKAG2 mutation. Additionally, a positive correlation occurred, associating reductions of both LVEF and RVFWLS.

We recognize limitations in the study, such as a relatively small number of patients. The software for obtaining RV4LS and RVFWLS was adapted from the software designed to measure the LV. Tricuspid regurgitation was detected in half of the study population, and increased systolic pulmonary pressure occurred in 4 patients, which was evaluated solely by this method.

Additional research using these criteria prospectively and the use of different imaging techniques for comparison are recommended to further validate our findings.

Conclusion

RV involvement in PRKAG2 is frequent and occurs in different degrees. Echocardiography is a valuable tool in detecting RV myocardial abnormalities in PRKAG2 cardiomyopathy. Two-dimensional RV4LS, RVFWLS, and 3D EF are reliable indicators of RV systolic dysfunction in this rare disease. Additional longitudinal studies are warranted to further understand the natural history of RV involvement and determine its impact on patient outcomes.

Author Contributions

Conception and design of the research: Pena JLB, Melo FJ, Santos WC, Moura I, Nakashima GP, Freitas NC, Sternick EB; Acquisition of data: Pena JLB, Santos WC, Moura ICG, Nakashima GP, Freitas NC, Sternick EB; Analysis and interpretation of the data and Writing of the manuscript: Pena JLB, Melo FJ, Santos WC, Moura ICG, Nakashima GP, Freitas NC, Sternick EB; Statistical analysis: Pena JLB,

Table 4 – Correlations between 3D RV EF and RV4LS and RVFWLS in all patients and those without and with a pacemaker

Group	Variable	3D RV EF	p-value
All patients	RV4LS	r = 0.445	0.018
	RVFWLS	r = 0.594	0.001
Without PM	RV4LS	r = 0.475	0.054
	RVFWLS	r = 0.654	0.006
With PM	RV4LS	r = 0.355	0.286
	RVFWLS	r = 0.533	0.091

EF: ejection fraction; PM: pacemaker; r: Spearman's correlation coefficient; RV: right ventricle; RV4LS: right ventricle longitudinal strain; RVFWLS: right ventricle free wall longitudinal strain; 3D: three-dimensional.

Table 5 – Intra- and interobserver data variability

	Intraobserver		Interobserver	
	Mean* (95% CI)	ICC (95% CI)	Mean* (95% CI)	ICC (95% CI)
RV4LS	0.4 (0.6; 1.5) ^{NS}	0.99 (0.93; 1.00) [†]	1.0 (2.0; 0.7) ^{NS}	0.98 (0.74; 1.00) [†]
RVFWLS	0.1 (2.4; 2.6) ^{NS}	0.94 (0.65; 0.99) [†]	0.4 (1.9; 2.7) ^{NS}	0.96 (0.75; 0.99) [†]
3D EF	1.3 (1.2; 3.9) ^{NS}	0.94 (0.66; 0.99) [†]	0.3 (2.5; 3.2) ^{NS}	0.93 (0.61; 0.99) [†]

*Mean of differences between intraobserver measurements (first and second measurements) and interobserver (observer 1 and observer 2 [collected study data]). CI: confidence interval; EF: ejection fraction; ICC: intraclass correlation coefficient; RV4LS: right ventricle longitudinal strain; RVFWLS: right ventricle free wall longitudinal strain; 3D: three-dimensional. [†]P-value < 0.05; NS P-value ≥ 0.05. All intra- and interobserver differences showed normal distribution, as assessed by the Shapiro-Wilk test.

Melo FJ, Santos WC, Moura ICG; Critical revision of the manuscript for important intellectual content: Pena JLB, Melo FJ, Moura I, Sternick EB.

Potential Conflict of Interest

No potential conflict of interest relevant to this article was reported.

Sources of Funding

There were no external funding sources for this study.

Study Association

This study is part of the thesis of master of Fabricio Junqueira de Melo by Faculdade Ciências Médicas de Minas Gerais

Ethics approval and consent to participate

This study was approved by the Ethics Committee of the Faculdade Ciências Médicas -MG under the protocol number 98623018.9.0000.5134. All the procedures in this study were in accordance with the 1975 Helsinki Declaration, updated in 2013. Informed consent was obtained from all participants included in the study.

References

- Lang T, Yu L, Tu Q, Jiang J, Chen Z, Xin Y, et al. Molecular cloning, genomic organization, and mapping of PRKAG2, a heart abundant gamma2 subunit of 5' AMP-activated protein kinase, to human chromosome 7q36. *Genomics*. 2000;70(2):258–63. doi: 10.1006/geno.2000.6376.
- Cheung PC, Salt IP, Davies PD, Hardie DG, Carling D. Characterization of AMP-activated protein kinase γ -subunit isoforms and their role in AMP binding. *Biochem J*. 2000;346(Pt 3):659–69. PMID:10698692
- Thevenon J, Laurent G, Ader F, Lafôret P, Klug D, Duva Pentiehl H, et al. High prevalence of arrhythmic and myocardial complications in patients with cardiac glycogenosis due to PRKAG2 mutations. *Europace*. 2017;19(4):651–9. doi: 10.1093/europace/euw067.
- Gollob MH, Green MS, Tang AS, Gollob T, Karibe A, Ali Hassan AS, et al. Identification of a gene responsible for familial Wolff-Parkinson-White syndrome. *N Engl J Med*. 2001;344(24):1823–31. doi:10.1056/NEJM200106143442403.
- Hardie DG, Carling D. The AMP-activated protein kinase—fuel gauge of the mammalian cell? *Eur J Biochem*. 1997;246(2):259–73. doi: 10.1111/j.1432-1033.1997.00259.x.
- Porto AG, Brun F, Severini GM, Losurdo P, Fabris E, Taylor MRG, et al. Clinical spectrum of PRKAG2 syndrome. *Circ Arrhythm Electrophysiol*. 2016;9(1):1–9. doi: 10.1161/CIRCEP.115.003121.
- Badano LP, Kolias TJ, Muraru D, Abraham TP, Aurigemma G, edvardsen T, et al. Standardization of Left Atrial, Right Ventricular, and Right Atrial Deformation Imaging Using Two-Dimensional Speckle Tracking. *Echocardiography: A Consensus Document of the EACVI/ASE/Industry Task Force to Standardize Deformation Imaging*. *Eur Heart J Cardiovasc Imaging*. 2018;19(6):591–600. doi: 10.1093/ehjci/jeu042.
- Maffessanti F, Muraru D, Esposito R, Gripari P, Ermacora D, Santoro C, et al. Age-, Body Size-, and Sex-Specific Reference Values for Right Ventricular Volumes and Ejection Fraction by Three-Dimensional Echocardiography: A Multicenter Echocardiographic Study in 507 Healthy Volunteers. *Circ Cardiovasc Imaging*. 2013;6(5):700–10. Doi:10.1161/CIRCIMAGING.113.000706
- Pena JLB, Santos WC, Siqueira MHA, Sampaio IH, Moura OCG, Sternick EB, et al. Glycogen storage cardiomyopathy (PRKAG2): diagnostic findings of standard and advanced echocardiography techniques. *Eur Heart J Cardiovasc Imaging*. 2021;22(7):800–7. doi: 10.1093/ehjci/jeaa176.
- Amsellem M, Mercier O, Kobayashi Y, Moneghetti K, Haddad F. Forgotten no more: a focused update on the right ventricle in cardiovascular disease. *JACC Heart Fail*. 2018 (11):891–903. doi: 10.1016/j.jchf.2018.05.022.
- Konstam MA, Kiernan MS, Bernstein DBozkurt B, Jacob M, Kapur NK, et al. Evaluation and management of right-sided heart failure: a scientific statement from the American Heart Association. *Circulation*. 2018;137(20):e578–e622. doi: 10.1161/CIR.0000000000000560.
- Pinsky MR. The right ventricle: interaction with the pulmonary circulation. *Crit Care*. 2016;20(1):266. doi: 10.1186/s13054-016-1440-0.
- Dell'Italia LJ. The right ventricle: anatomy, physiology, and clinical importance. *Curr Probl Cardiol*. 1991;16(10):653–720. doi: 10.1016/0146-2806(91)90009-y
- Petitjean C, Rougon N, Cluzel P. Assessment of myocardial function: a review of quantification methods and results using tagged MRI. *J Cardiovasc Magn Reson*. 2005;7(2): 501–16. doi: 10.1081/jcmr-200053610
- Lang RM, Badano LP, Mor-Avi V, Afilalo J, Armstrong A, Ernande L, et al. Recommendations for cardiac chamber quantification by echocardiography in adults: an update from the American Society of Echocardiography and European Association of Cardiovascular Imaging. *J Am Soc Echocardiogr*. 2015;28(1):1–39.e14. doi: 10.1016/j.echo.2014.10.003.
- Rudski LG, Lai WW, Afilalo J, Hua L, Handschumaker MD, Chandrasekaran K, et al. Guidelines for the Echocardiographic Assessment of the Right Heart in Adults: A Report from the American Society of Echocardiography endorsed by the European Association of Echocardiography, a Registered Branch of the European Society of Cardiology, and the Canadian Society of Echocardiography. *J Am Soc Echocardiogr*. 2010;23(7):685–713. doi: 10.1016/j.echo.2010.05.010.
- Hu D, Hu D, Liu L, Barr D, Liu Y, Valderrabano-Saucedo N, et al. Identification, Clinical Manifestation and Structural Mechanisms of Mutations in AMPK Associated Cardiac Glycogen Storage Disease. *EBioMedicine*. 2020;54:102723. doi: 10.1016/j.ebiom.2020.102723.
- Thevenon J, Laurent G, Ader F, Lafôret P, Klug D, Pentiehl AD, et al. High prevalence of arrhythmic and myocardial complications in patients with cardiac glycogenosis due to PRKAG2 mutations. *EP Europace*. 2017;19(4):651–9. doi:10.1093/europace/euw067.
- Sternick EB, Oliva A, Gerken LM; Magalhães L, Scarpelli R, Correia FS, et al. Clinical, electrocardiographic, and electrophysiologic characteristics of patients with a fasciculoventricular pathway: the role of PRKAG2 mutation. *Heart Rhythm*. 2011;8(1):58–64. doi: 10.1016/j.hrthm.2010.09.081.
- Lopez-Sainz A, Dominguez F, Lopes LR, Ochoa JP, Barriales-Villa R, Climent V, et al. Clinical features and natural history of PRKAG2 variant cardiac glycogenosis. *J Am Coll Cardiol*. 2020;76(2):186–97. doi: 10.1016/j.jacc.2020.05.029.
- Sanz J, Sánchez-Quintana D, Bossone E, Bogaard H, Meije R. Anatomy, Function, and Dysfunction of the Right Ventricle: JACC State-of-the-Art Review. *J Am Coll Cardiol*. 2019;73(12):1463–82. doi: 10.1016/j.jacc.2018.12.076.
- Maron BJ. Clinical Course and Management of Hypertrophic Cardiomyopathy. *N Engl J Med*. 2018;379(7):855–68. doi: 10.1056/NEJMra1710575.
- Roşca M, Călin A, Beladan CC, Enache R, Meetesu AD, Gurzun MN, et al. Right ventricular remodeling, its correlates, and its clinical impact in hypertrophic cardiomyopathy. *J Am Soc Echocardiogr*. 2015;28(11):1329–38. Doi:10.1016/j.echo.2015.07.015.

24. Moñivas Palomero V, Durante-Lopez A, Sanabria MT, Cubero JS, Gonzalez-Mirelis J, Lopez-Ibor JV, et al. Role of Right Ventricular Strain Measured by Two-Dimensional Echocardiography in the Diagnosis of Cardiac Amyloidosis. *J Am Soc Echocardiogr.* 2019;32(7):845-53. e1. doi: 10.1016/j.echo.2019.03.005.
25. Ahmed M, Gorcsan J 3rd, Marek J, Ryo K, Haugaa K, R Ludwig D, et al. Right ventricular apical pacing-induced left ventricular dyssynchrony is associated with a subsequent decline in ejection fraction. *Heart Rhythm.* 2014;11(4):602-8. doi: 10.1016/j.hrthm.2013.12.020.
26. Nagata Y, Wu VC, Kado Y, Otani K, Lin FC, Otsugi Y, et al. Prognostic Value of Right Ventricular Ejection Fraction Assessed by Transthoracic 3D Echocardiography. *Circ Cardiovasc Imaging.* 2017;10(2):e005384 doi:10.1161/CIRCIMAGING.116.005384.
27. Morris DA, Blaschke D, Canaan-Kühl S, Plockinger U, Knobloch G, Walter TC, et al. Global cardiac alterations detected by speckle-tracking echocardiography in Fabry disease: left ventricular, right ventricular, and left atrial dysfunction are common and linked to worse symptomatic status. *Int J Cardiovasc Imaging.* 2015 Feb;31(2):301-13. doi: 10.1007/s10554-014-0551-4.
28. Yogasundaram H, Paterson ID, Graham M, Sergi C, Oudit GY, et al. Glycogen storage disease because of a PRKAG2 mutation causing severe biventricular hypertrophy and high-grade atrio-ventricular block. *Circ Heart Fail.* 2016;9(8):e003367. doi: 10.1161/CIRCHEARTFAILURE.116.003367.

